Connaughton and Dabagh
BioMedical Engineering OnLine (2024) 23:88
https://doi.org/10.1186/s12938-024-01278-0

BioMedical Engineering OnLine

RESEARCH Open Access

Impact of stroma remodeling on forces experienced by cancer cells and stromal cells within a pancreatic tumor tissue

Morgan Connaughton[1] and Mahsa Dabagh[1*]

*Correspondence:
dabaghme@uwm.edu

[1] Department of Biomedical Engineering, University of Wisconsin-Milwaukee, Milwaukee, WI 53211, USA

Abstract

Remodeling (re-engineering) of a tumor's stroma has been shown to improve the efficacy of anti-tumor therapies, without destroying the stroma. Even though it still remains unclear which stromal component/-s and what characteristics hinder the reach of nanoparticles deep into cancer cells, we hypothesis that mechanisms behind stroma's resistance to the penetration of nanoparticles rely heavily on extrinsic mechanical forces on stromal cells and cancer cells. Our hypothesis has been formulated on the basis of our previous study which has shown that changes in extracellular matrix (ECM) stiffness with tumor growth influence stresses exerted on fibroblasts and cancer cells, and that malignant cancer cells generate higher stresses on their stroma. This study attempts to establish a distinct identification of the components' remodeling on the distribution and magnitude of stress within a tumor tissue which ultimately will impact the resistance of stroma to treatment. In this study, our objective is to construct a three-dimensional in silico model of a pancreas tumor tissue consisting of cancer cells, stromal cells, and ECM to determine how stromal remodeling alters the stresses distribution and magnitude within the pancreas tumor tissue. Our results show that changes in mechanical properties of ECM significantly alter the magnitude and distribution of stresses within the pancreas tumor tissue. Our results revealed that these stresses are more sensitive to ECM properties as we see the stresses reaching to a maximum of 22,000 Pa for softer ECM with Young's modulus of 250 Pa. The stress distribution and magnitude within the pancreas tumor tissue does not show high sensitivity to the changes in mechanical properties of stromal cells surrounding stiffer cancer cells (PANC-1 with Young's modulus of 2400 Pa). However, softer cancer cells (MIA-PaCa-2 with (Young's modulus of 500 Pa) increase the stresses experienced by stiffer stromal cells and for stiffer ECM. By providing a unique platform to dissect and quantify the impact of individual stromal components on the stress distribution within a tumor tissue, this study serves as an important first step in understanding of which stromal components are vital for an efficient remodeling. This knowledge will be leveraged to overcome a tumor's resistance against the penetration of nanoparticles on a per-patient basis.

Keywords: Pancreatic cancer, Remodeling, Stroma, ECM, Stresses within tumor, Cancer treatment

Introduction

Pancreatic cancer is one of most prevalent type of cancer which is expected to become the second leading cause of cancer death in the United States by 2030 [1]. Pancreatic cancer is often lethal, with 1-year and 5-year survival rates at 24% and 8%, respectively [1]. The low survival rate in patients with pancreatic cancer is mainly due to the formation of a dense and fibrotic barrier by the tumor stroma that literally blocks the penetration of drugs deep into the cancer cells [2–10]. The stroma structurally consists of fibroblasts, a basement membrane matrix, an extracellular matrix (ECM), immune cells, and a vasculature that evolves over time and varies in patients [2–16]. Although our knowledge of the malignant pancreatic cancer and their resistance to drug therapies continually improves, the mechanisms involved in overcoming resistance of tumors to therapies principally remain a mystery. We very well know that cancer cells alter their stroma to support their growth and proliferation [4, 10–16]. Furthermore, we know that remodeling (re-engineering) of stroma can improve the efficacy of anti-tumor therapies, rather than destroying the stroma [2–35].

In the last 2 decades, several models––including in vitro, in vivo, ex vivo, and mathematical (and numerical and cell-based computational)––have been developed to improve the understanding of cancer treatment resistance and to use this knowledge for personalized treatment [2–35]. However, these models have faced serious challenges mainly because they have not been successful in reconstructing human tumor tissue. This is mainly due to tumor stroma being highly heterogeneous; it changes by tumor growth, and its components and proportion changes inter/intra-personally [2–35]. Patient-derived in vitro models of human cancer were very promising and were supposed to overcome key challenges of in vivo models. However, their turnaround time has not been adequate for clinical application. Furthermore, in in vitro models, including 2D/3D cell culture and 3D bioprinting, the main challenge is still in modeling of appropriate ECM for pancreatic cancer [2–35]. Thus, ex vivo models have been developed with the promise of recapitulating in vivo tumor biology [4, 9, 14]. On the other hand, the biggest challenge in translating results of mathematical models to human clinical studies stems from the fact they are not calibrated to a particular type of cancer [17–32]. These models mostly apply the same criteria for tumor regression patterns associated with treatment across a wide range of tumor types, and differences between tumor sites and treatment modalities are not considered [19, 23, 29–32]. Another major challenge translating the results of these models to clinical studies is that they are based on goodness-of-fit criteria to data from a pre-clinical experiment; thus, they may not provide the most accurate predictions of treatment outcomes in humans [17–32]. Furthermore, these models apply a population estimate approach that cannot provide prognostic insights and are limited in offering treatment options at the patient level [19, 23, 29–32]. Cell-based computational models, which explore individual cell behaviors within tissue environments by simulating individual cells interacting with virtual tissues, constrain the flexibility of cell shape and diameter [23, 31, 32]. Most cell-based models couple a discrete model to continuum models of the microenvironment whereas the transport of drug and other species are simulated using partial differential equations [23, 32]. Taking all together, utilizing patient-specific tumor dynamics, rather than using tumors that are not patient-derived, to predict the response to treatment will enhance the sensitivity and

accuracy of computational models. However, for personalized treatment, deeper understanding of tumor physiology and dynamics is required. This demands the incorporation of tumor tissue's cellular heterogeneity into the computational models. Recently, we reconstructed an idealized model of a tumor tissue representing three different organs including breast, kidney, and pancreas where they integrated patient-specific characteristics of ECM, stroma, and cancer cells [36]. They reported that (A) the stresses within tumor tissue are impacted by the organ-specific ECM's biophysical properties, (B) more invasive cancer cells experience higher stresses, (C) in pancreas which has a softer ECM (Young's modulus of 1.0 kPa) and stiffer cancer cells (Young's modulus of 2.4 kPa and 1.7 kPa) than breast and kidney, cancer cells experienced significantly higher stresses, and (D) cancer cells in contact with ECM experienced higher stresses compared to cells surrounded by fibroblasts but the area of tumor stroma experiencing high stresses has a maximum length of 40 μm when the cancer cell is surrounded by fibroblasts and 12 μm for when the cancer cell is in vicinity of ECM. Based on these findings, we are interested to reveal how these significantly high stresses in pancreas will impact the treatment process. In this study, we take the first step in developing an idealized in silico model of pancreas tumor tissue to dissect and understand how remodeling of each stromal components can impact the stress distribution within the pancreas tumor. Without a distinct identification of the components' remodeling on the distribution and magnitude of stress within pancreas tumor tissue which directly impacts the resistance of stroma to nanoparticles' penetration, all attempts to improve drug therapies' success will remain out of reach.

Nanoparticles have shown to be an effective drug-delivery platform that enhanced permeability and retention (EPR) by passively targeting the tumor [37]. Mechanisms that impede nanoparticles' penetration within stroma are still under debate because stroma is highly heterogeneous but the inability of nanoparticles to correctly target the tumor, limited permeability of nanoparticles within tumor stroma, and nanoparticles non-uniform distributions in solid tumor tissue should all be considered as limiting factors. A study conducted by Ernstring et al., analyzed Cellax nanoparticles treatment effects in highly stromal primary patient-derived pancreatic cancer xenografts and in a metastatic PAN02 mouse model of pancreatic cancer [38]. They found that Cellax nanoparticles were able to deplete CAFs and that the depletion of stroma density led to > tenfold increase in tumor perfusion, reduced tumor weight and a reduction in metastasis. Even though nanoparticles have been shown to be quite promising in mouse models, but it has been shown that variation between organ-specific tumors affect EPR differently and that eliminating the stroma barrier is quite complex. This has led to failed clinical trials for nanotherapeutics [2, 38]. Furthermore, the extreme depletion of the tumor stroma has been reported to promote tumor progression, therefor, finding the balance between abundance and depleted stroma would be highly beneficial to pancreatic cancer treatments [2, 39]. Several characteristics of stroma have been reported to be altered during its remodeling such as (A) fibroblasts' shape, size, stiffness, permeability, (B) ECM's stiffness, density, and plasticity, and (C) crosslinking of collagens [40, 41]. Therefore, understanding how biomechanical factors are changing during stroma remodeling will assist us with precise design of nanoparticles capable of remodeling of tumor stroma instead of eliminating CAFs. The purpose of the present study is to use an in silico model of

idealized pancreas tumor tissue to quantify the stress experienced by the stromal and cancer cells during remodeling process induced by stroma-targeted drug-therapy. Our model will also provide better understanding of the mechanical interactions between stromal cells and cancer cells during the remodeling.

Results

Influence of ECM remodeling on stress distribution within pancreatic tumor tissue

Figure 1 demonstrates the von Mises stress magnitude within the pancreas tumor tissue with the assumption that tumor remodeling has reflected in changes in ECM stiffness. Figures 1A and D show the stresses along the tissue width (x-axis) where the analysis domain is limited to the cancer cells' thickness (y-axis) and length (z-axis); Figs. 1B and

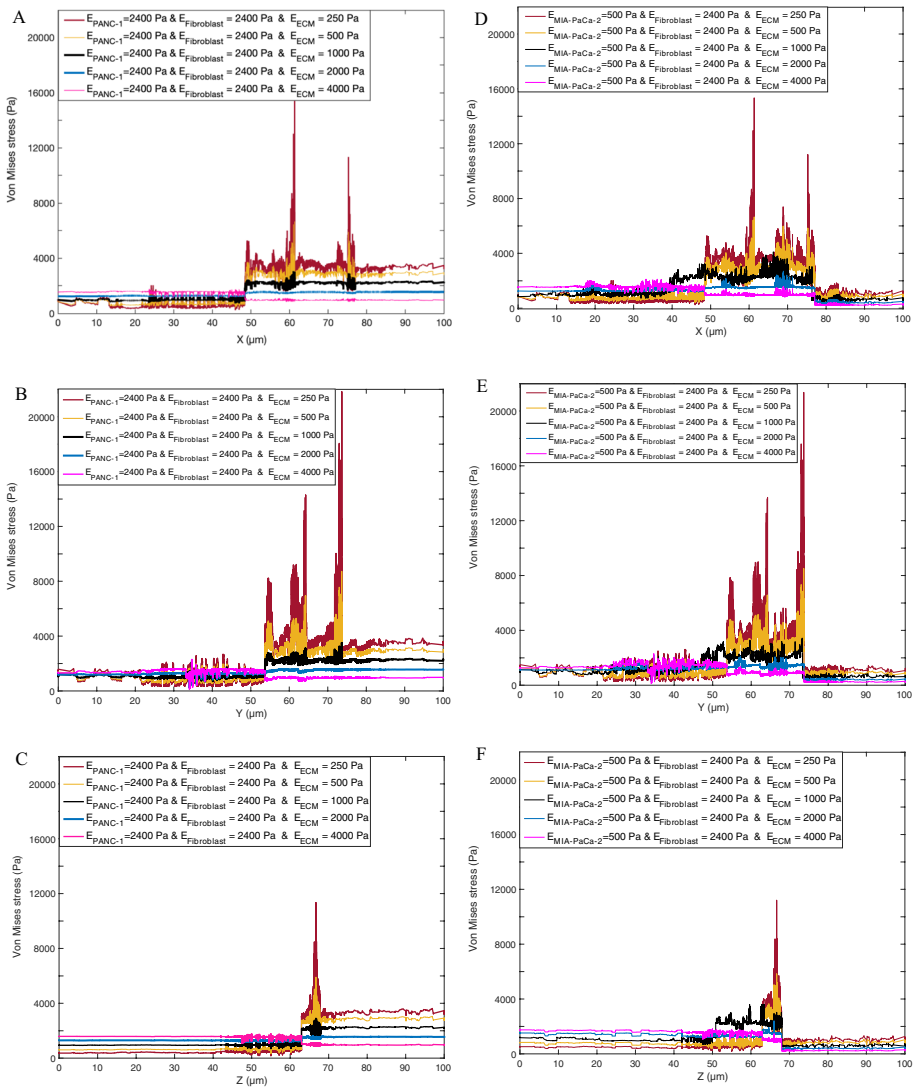

Fig. 1 The von Mises stress magnitude within the pancreas tumor tissue, A and D) the stresses along the tissue width (x-axis), B and E) the stresses along the tissue thickness (y-axis), C and F) the stresses along the tissue length (z-axis). Note that these results represent in silico model of the pancreatic tumor tissue with three cancer cells

E demonstrates the stresses along the tissue length (y-axis) where the analysis domain is limited to the cancer cells' width (x-axis) and length (z-axis); Figs. 1C and F show the stresses along the tissue thickness (z-axis) where the analysis domain is limited to the cancer cells' width (x-axis) and thickness (y-axis). In Figs. 1A–C, three PANC-1 are surrounded by ECM and stromal cells while three MIA-PaCa-2 are surrounded by ECM and stromal cells in Figs. 1D–E.

Influence of stroma and ECM remodeling on stress distribution within pancreatic tumor tissue

Figure 2 demonstrates the von Mises stress magnitude within the pancreas tumor tissue with the assumption that tumor remodeling has reflected in changes in ECM and stroma

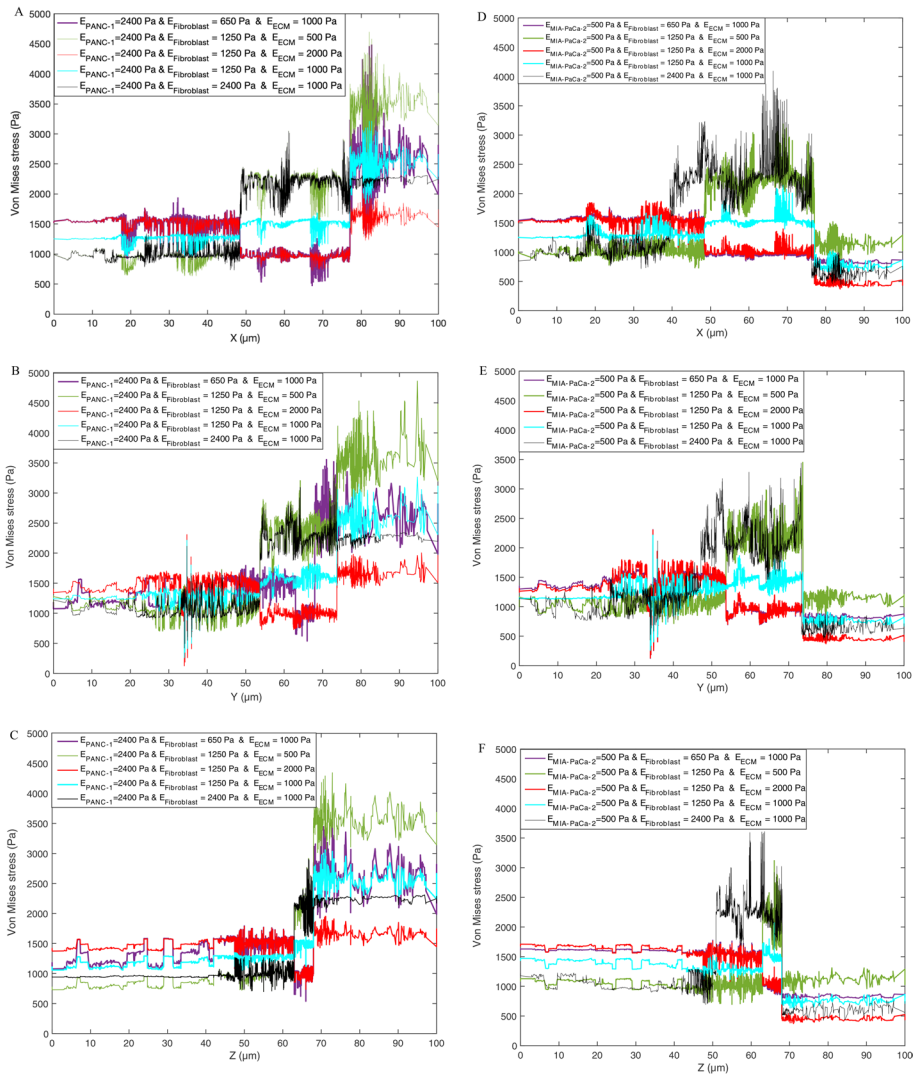

Fig. 2 The von Mises stress magnitude within the pancreas tumor tissue, A and D) the stresses along the tissue width (x-axis), B and E) the stresses along the tissue thickness (y-axis), C and F) the stresses along the tissue length (z-axis). Note that these results represent in silico model of the pancreatic tumor tissue with three cancer cells

stiffness. Figures 2A and D show the stresses along the tissue width (x-axis); Figs. 2B and E demonstrate the stresses along the tissue thickness (y-axis); Figs. 2C and F show the stresses along the tissue length (z-axis). In Figs. 2A–C, three PANC-1 are surrounded by ECM and stromal cells while three MIA-PaCa-2 are surrounded by ECM and stromal cells in Figs. 2D–E.

Figures 3A–R show the von Mises stress and the strain distribution within a pancreas tumor with three cancer cells. In each panel, there are three parts showing: (i) the stresses along the tissue width (x-axis), (ii) the stresses along the tissue length (z-axis), and (iii) the strain along the tissue width (x-axis).

Figure 4 demonstrates the von Mises stress magnitude averaged over whole tumor tissue with three cancer cells. In Fig. 4A, cancer cells have a Young's modules of 2400 Pa while in Fig. 4B cancer cells have a Young's modules of 500 Pa. The x-axis is the ratio of fibroblast's stiffness to ECM's stiffness.

Figure 5A shows a new model where the stroma is extended over the whole width of the ECM. Figures 5B–D demonstrate the stresses along the tissue width (x-axis), the tissue thickness (y-axis); and along the tissue length (z-axis), respectively.

Influence of remodeling on the stress distribution within a pancreas tumor with higher number of cancer cells

Figure 6A–F demonstrate the von Mises stress magnitude within the pancreas tumor tissue when higher cancer cells are included. Here, we examine how the stress distribution will vary when the remodeling induces changes in both, the stiffness of tumor stroma and ECM. Figures 6A and D show the stresses along the tissue width (x-axis); Figs. 6B and E demonstrate the stresses along the tissue thickness (y-axis); Figs. 6C and F show the stresses along the tissue length (z-axis). Figure 7 demonstrates the von Mises stress magnitude within the pancreas tumor tissue with the assumption that tumor remodeling has reflected in changes in ECM and stroma stiffness. Figures 7A and D show the stresses along the tissue width (x-axis); Figs. 7B and E demonstrate the stresses along the tissue thickness (y-axis); Figs. 6C and 7F show the stresses along the tissue length (z-axis). In Figs. 6A–C and 7A–C, three PANC-1 are surrounded by ECM and stromal cells while three MIA-PaCa-2 are surrounded by ECM and stromal cells in Figs. 6D–E and 7D–E.

Discussion

In this study, we have developed an in silico model of a pancreas tumor tissue and applied it to investigate how remodeling of tumor tissue components will impact the stress magnitude exerted on their surroundings. Mechanical forces exerted on cancer cells by their microenvironment have been reported to drive cells toward invasive phenotype by altering cells' motility, proliferation, and apoptosis. It has been shown that the mechanical forces, if sufficiently strong, may contribute to loss of membrane integrity, for instance through tumor-induced enzymatic digestion of ECM [58]. These forces emanating from overlying differentiated tumor cells may mechanically drive the invasion of tumor-initiating progenitors at the stromal border. The stroma has been reported to play a significant role in shaping tumor architecture by altering inherent patterns of tumor glands in human pancreas [59]. On the other hand, the failure of most standard

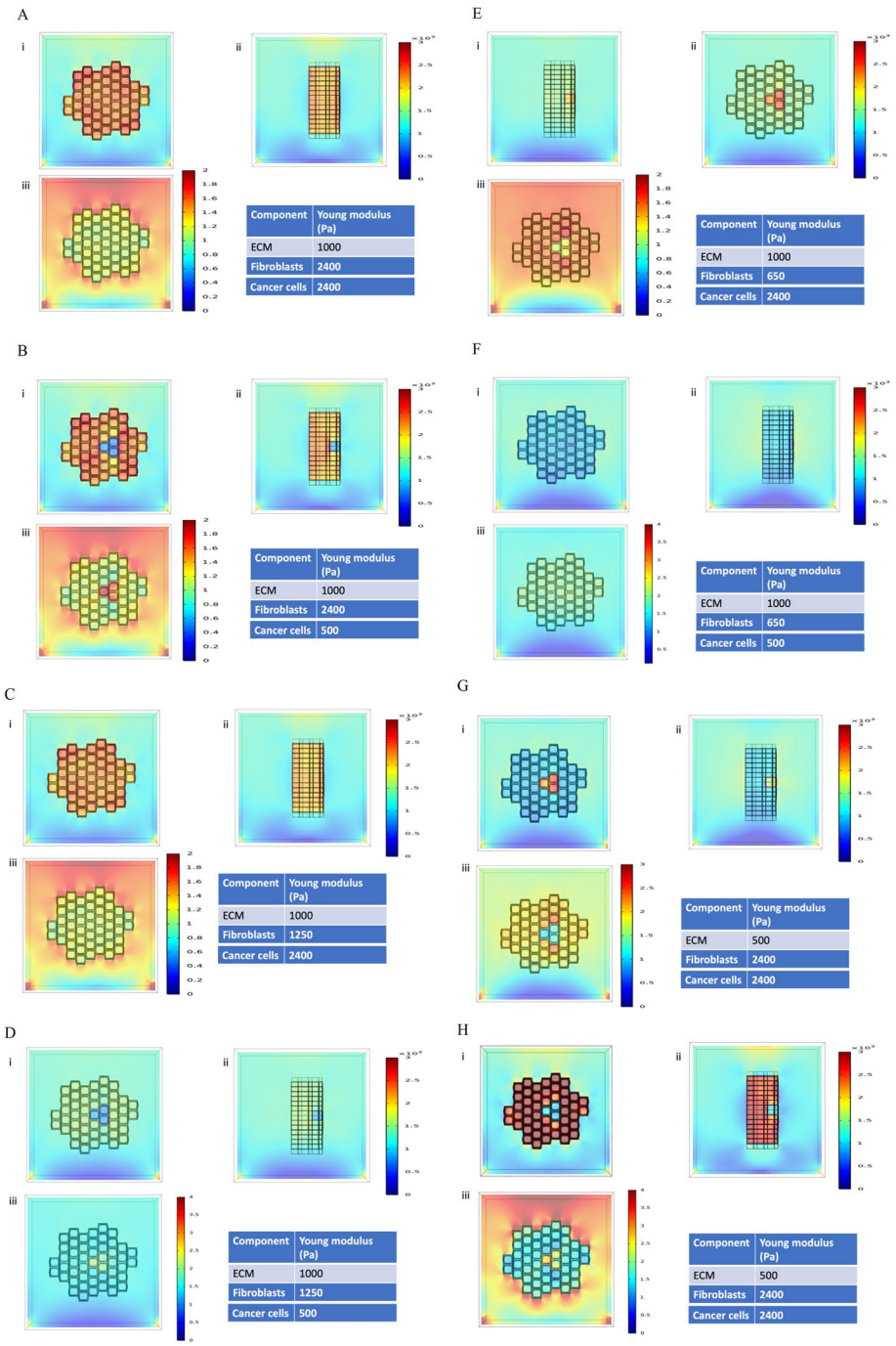

Fig. 3 The von Mises stress distribution within the pancreas tumor tissue. i) the stresses (Pa) along the tissue width (x-axis), ii) the stresses (Pa) along the tissue length (z-axis), iii) the strain along the tissue width (x-axis)

therapies in pancreatic cancer, as well as promising immune therapies, rely heavily on highly unique and protective stromal microenvironments presenting significant biophysical barriers to effective drug delivery [60]. Our in silico model of pancreas tumor tissue enabled us to dissect and quantify the role of each tissue components' remodeling on the stress distribution within a pancreas tumor tissue. Previous studies have shown

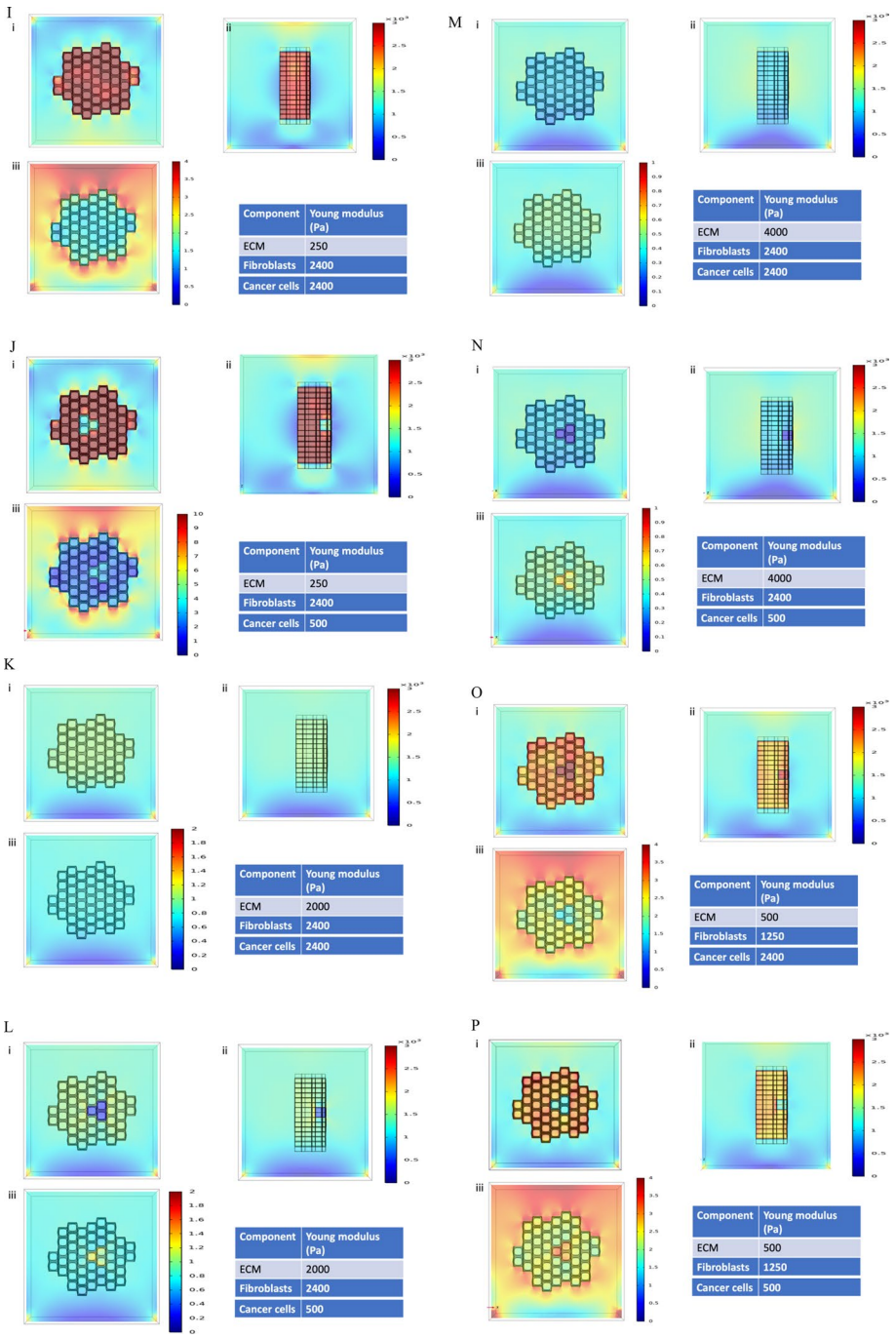

Fig. 3 continued

that extreme depletion of the tumor stroma promotes tumor progression, therefore, finding the balance between abundance and depleted stroma would be highly beneficial to pancreas tumor treatments [39]. On the other hand, nanoparticles have shown the capability to remodel stroma and ECM, rather than destroying fibroblasts and collagen fibers. Stiffness of tumor stroma and ECM are among several examined parameters which have been reported to be altered during remodeling and impact cancer cells

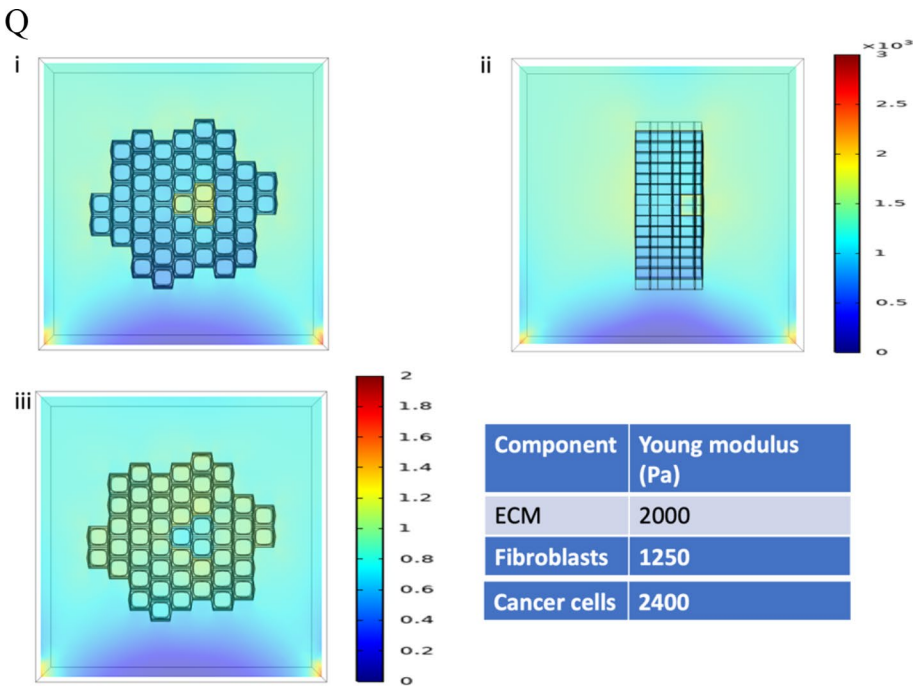

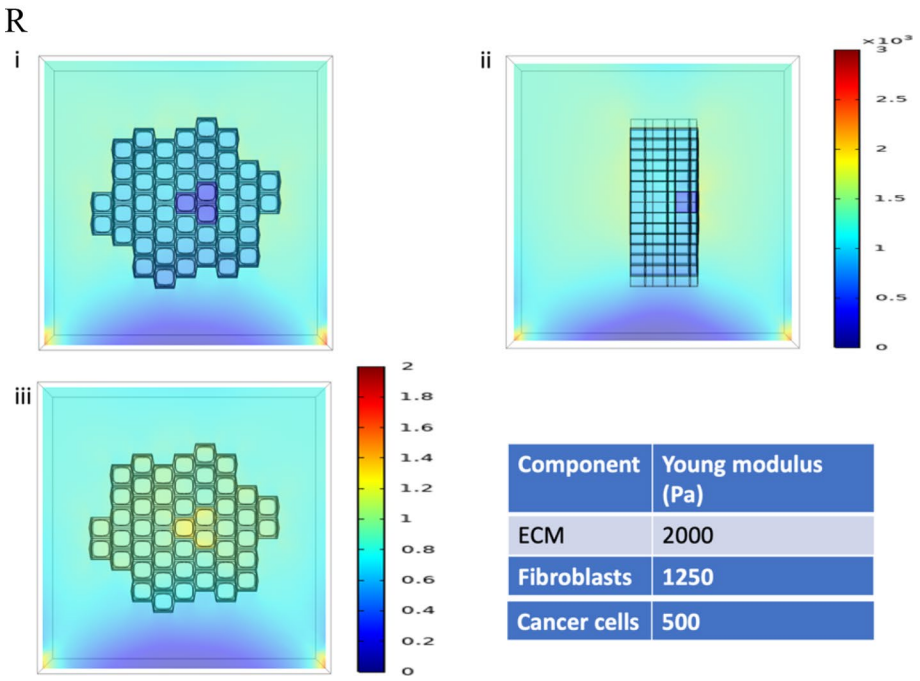

Fig. 3 continued

growth [4, 7, 41, 61]. Therefore, we have examined the impact of remodeling-induced-alteration in the stiffness of both the ECM and stroma on stress distribution within the pancreas tumor tissue. In addition, we have investigated whether number of cancer cells in the tumor may change the impact of ECM and stroma remodeling on stress distribution with the pancreatic tumor tissue.

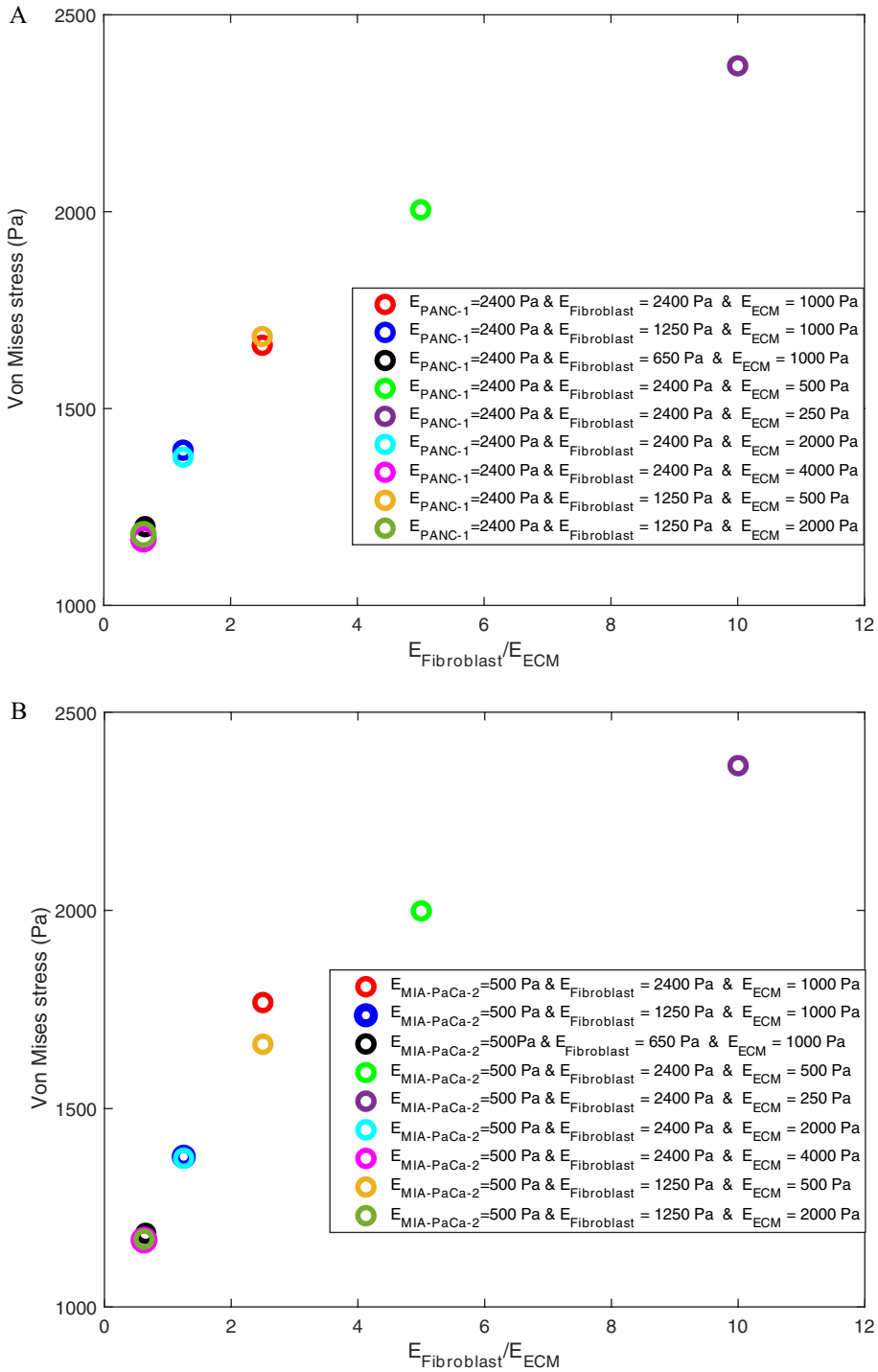

Fig. 4 The averaged von Mises stress values over whole tumor tissue. Note that the tumor has three cancer cells

Our results (Figs. 1, 2, 3, 4, 5, 6 and 7) show that the remolding-induced-changes in ECM and stroma stiffness impact the von Mises stress distribution within the pancreatic tumor tissue. Soft ECM with stiffness of < 1000 Pa when surrounded with soft stroma and cancer cells results in dramatically high stresses within the pancreas tumor tissue. In

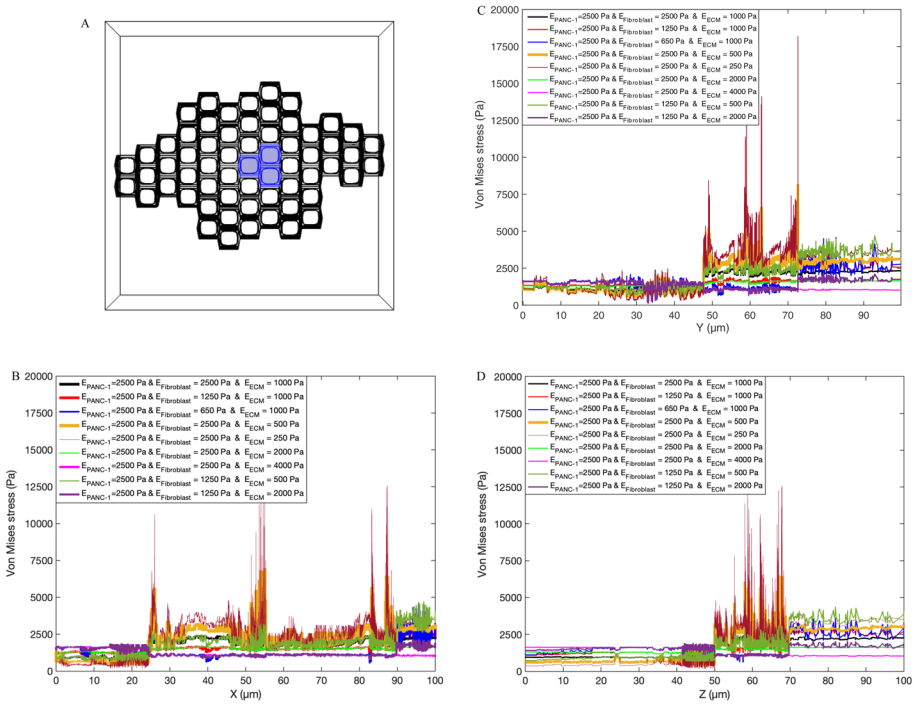

Fig. 5 A) In silico model of the pancreas tumor tissue containing stromal cells and three tumor cells, and ECM. In this model, the stroma is extended along whole width of the ECM. B-D): The von Mises stress magnitude within the pancreas tumor tissue, B) the stresses along the tissue width (x-axis), C) the stresses along the tissue thickness (y-axis), D) the stresses along the tissue length (z-axis). Note that these results represent in silico model of the pancreatic tumor tissue with three cancer cells

softer ECM (Young's modulus of 250 Pa), the stresses reach to a maximum of 22,000 Pa (shown in Figs. 1B). Furthermore, Figs. 1A–C show that when ECM becomes softer (e.g., when ECM's stiffness drops below 1000 Pa) and stroma has similar stiffness as the cancer cells, the stresses within pancreas tumor tissue are increasing dramatically. With ECM becoming very soft (Young's modulus of 250 Pa), the stresses jump dramatically to reach a maximum of 11,000, 22,000, and 16,000 Pa for results as seen in Figs. 1A–C. The data shown in these figures reveal the fact that the increase in the stress magnitude within the pancreas tumor tissue with ECM softening is not linear. Figures 1D–E demonstrate that, in tumor tissue with softer cancer cells (MIA-PaCa-2), ECM and stromal cells experience slightly higher stresses, particularly when ECM is stiffer. Results shown in Fig. 2A–C demonstrate the fact that softening of stroma doesn't significantly rise the stress magnitude in the tumor tissue. However, stroma's stiffness becomes more influential when cancer cells become softer. Our results (Figs. 2D–F) show that softer cancer cells (MIA-PaCa-2) causes to higher stresses within ECM and stroma specifically when stromal cells are stiffer. Figures 3 represents the stress distribution over the tumor microenvironment through a visual representation of the stresses with respect to the changing microenvironment stiffness. A comparison between Figs. 1, 2, 3, 4, 5, 6 and 7 demonstrates that changes in the stresses magnitude and distribution within pancreas tumor tissue due to cancer cells and ECM's stiffness is significantly higher than tumor stroma. When the stroma softens, the stresses rise but not significantly (Figs. 2A–F

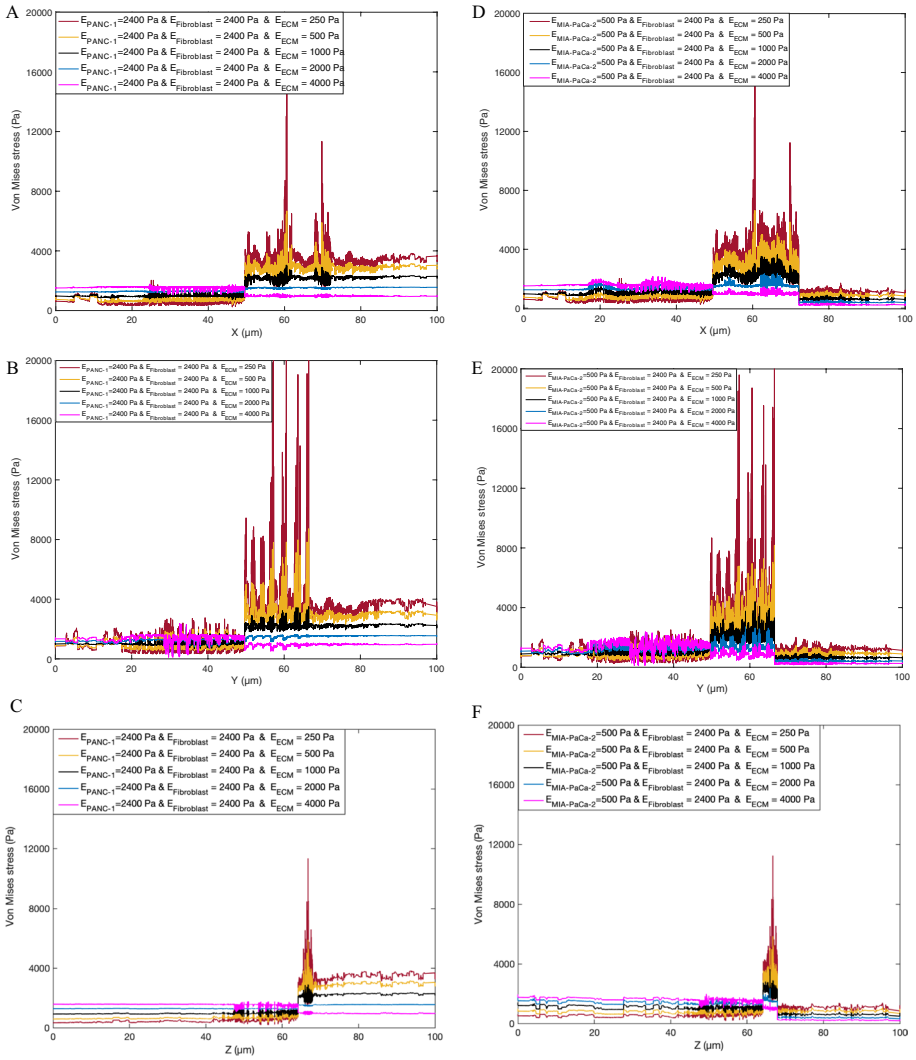

Fig. 6 The von Mises stress magnitude within the pancreas tumor tissue, A and D) the stresses along the tissue width (x-axis), B and E) the stresses along the tissue thickness (y-axis), C and F) the stresses along the tissue length (z-axis). Note that these results represent in silico model of the pancreatic tumor tissue with nine cancer cells

and Figs. 7A–F). Figure 3 reveals that the stiffness of ECM and cancer cells significantly impacts the strain distribution within the pancreas tissue significantly. Higher strain magnitude is observed for a tumor tissue with softest ECM (Young's modulus of 250 Pa) and softer cancer cells (MIA-PaCa-2). Lower stresses and strains are observed for stiffest ECM (Young's modulus of 4000 Pa) and stiffer cancer cells (PANC-1). Figure 5 shows that extending the stroma to the whole width of the stroma leads to more uniform increase across the ECM and larger areas of the tumor experiences higher stresses particularly for softer ECM. Figures 6 and 7 confirm that the tumor's size alters the response of tumor tissue to remodeling-induced-alteration in stroma and ECM. While in smaller tumors the stroma softening seems to have ignorable impact on the stresses experienced by tumor tissue, it shows a significant influence in a larger tumor. On the other hand, ECM's stiffness is not showing dependency on the tumor size. Our findings still need to

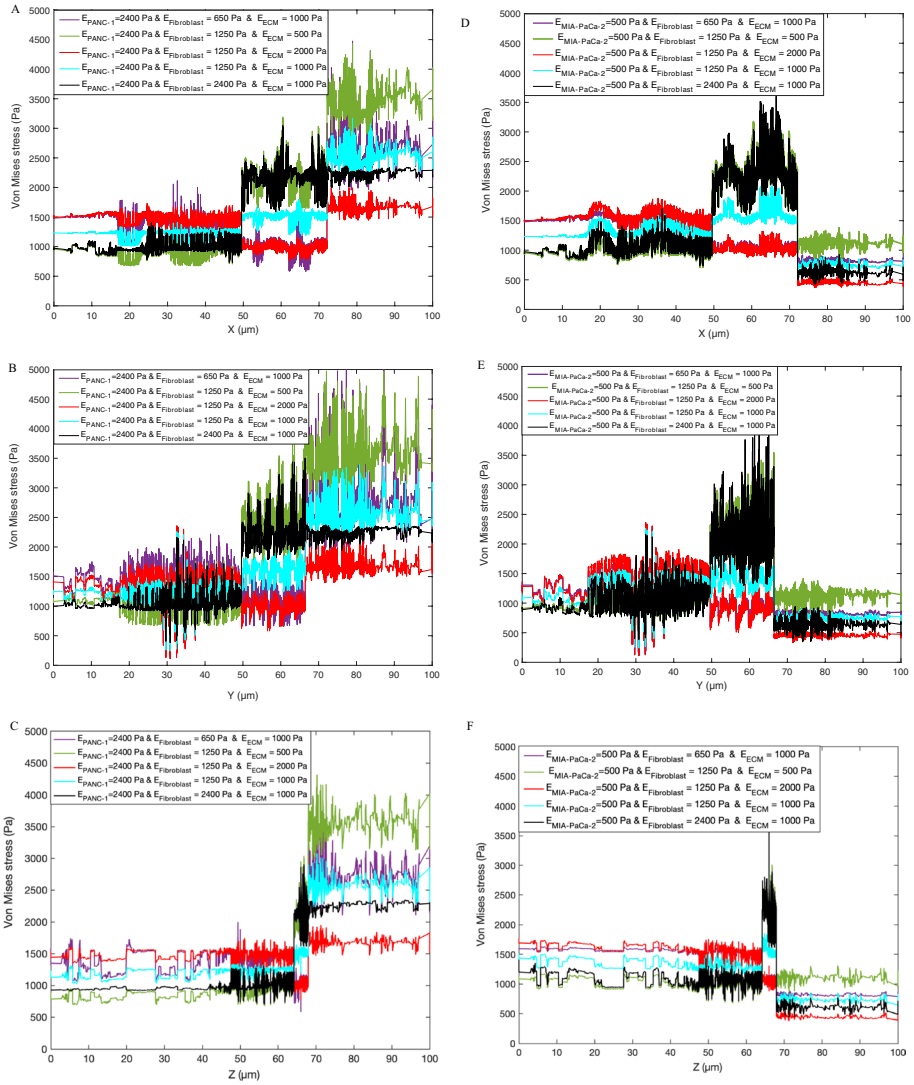

Fig. 7 The von Mises stress magnitude within the pancreas tumor tissue, A and D) the stresses along the tissue width (x-axis), B and E) the stresses along the tissue thickness (y-axis), C and F) the stresses along the tissue length (z-axis)

be validated with in vivo experiments to allow us to reach a general conclusion, but we show, in agreement with previously reported studies, that tumor size and stresses experienced by the tumor tissue components may be introduced as key biomarkers to predict a patient-specific tumor's response to a particular treatment [62–71].

Our study has a few limitations: (A) the three-dimensional in silico model of pancreas tumor tissue did not fully represent the patient-specific complexity of the cellular microenvironment, (B) ECM was assumed as a homogeneous media not including important microvascular structures seen within the ECM, such as fiber-forming elements (collagen and elastin) surrounded by various filling molecules (glycoproteins and proteoglycans), growth factors, and adhesion molecules, and (C) modeling fibroblasts as a hexagon, as these cells are often elongated and spindle-shaped, (D) this in silico model of microenvironment also did not consider vessels present in tumor microenvironment which is

because of the limitations in currently available imaging techniques not detecting small vessels formed in the tumor microenvironment. Nonetheless, we have been able to gain important quantified insights on the extrinsic mechanical forces on stromal cells and cancer cells and how these forces can be controlled by remodeling of tumor components. Here, we take the first step in developing a unique platform for building an idealized, in silico model of pancreas tumor tissue to dissect and understand how remodeling of each stromal components can impact the stress distribution within a pancreas tumor tissue. Our findings can be applied in developing patient-specific in silico models of different tumor types to design efficient remodeling strategies per patient basis. Developing patient-specific in silico models of different organs with tumor types at distinct states of malignancy will require advanced imaging methods (such as standard and high definition Fourier Transform Infrared (FTIR) imaging) being capable of acquiring stromal diversity.

Conclusion

This study serves as an important first step in understanding of how the remodeling of tumor tissues' components impact the pancreas tumor tissue and which components are vital for an efficient remodeling, by developing an in silico model of pancreas tumor tissue to dissect and quantify the impact of individual components on the stress distribution within a pancreas tumor tissue. Our results show that the remodeling of stroma and ECM will alter the distribution and magnitude of stresses within tumor tissue. Our study reveals that the remodeling induced softening of ECM has higher impact on the stress magnitude and distribution within the PDASC tissue than softening of stromal cells. Our results also show that stiffness of cancer cells in a tumor impacts the stresses experienced by ECM and the stroma, but this impact is significant when stroma is stiffer. These results confirm our hypothesis that mechanisms behind stroma's resistance to the penetration of nanoparticles rely heavily on extrinsic mechanical forces on stromal cells and cancer cells. As a debatable matter, mechanisms impeding nanoparticles in reaching cancer cells are at the central attention, specifically by noting that stroma is highly heterogeneous, inter-/intra-personally, affected by tumor malignancy. To our knowledge, this is the first study on quantifying the impact of tumor tissue components' remodeling, and it will serve as an important first step in establishing unique knowledge on the characteristic factors for remodeling of tumor microenvironment's components with an ultimate goal of leveraging this knowledge to overcome a tumor's resistance against the penetration of nanoparticles on a per-patient basis. The three-dimensional, multicomponent, in silico model used in the present study has the potential to further study highly complex tumor microenvironments in cancers that are severely understudied and will bring light to critical role of physical stresses on tumor growth and understanding of complex mechanisms involved in a tumor's response to drugs and precise assessment of alternative drugs.

Methods

In the present study, the geometric model included cancer cells, stromal cells represented as fibroblasts, and the ECM, as seen in Fig. 8A and B. Cancer cell and fibroblasts are represented as a hexagonal shape with length of 8.1 μm (X-axis), a width of

7.54 μm (Y-axis), and a height of 8.0 μm (Z-axis) to mimic the size of a typical cells [42–45]. The ECM is modeled as a viscoelastic material using the Standard Linear Model with the following paraments [46, 47]: Young's modulus (E) = 250 Pa, shear modulus (G) = 63.3 Pa, bulk modulus (K) = 8333.3 Pa, Viscoelasticity relaxation time (T) = 0.2245 s; E = 500 Pa, G = 167.2 Pa, K = 16666.6 Pa, T = 0.449 s; E = 1000 Pa, G = 334.4 Pa, K = 33333.3 Pa, T = 0.898 s; E = 2000 Pa, G = 668.89 Pa, K = 66666.6 Pa, T = 1.796 s; E = 4000 Pa, G = 1337.79 Pa, K = 133333.3 Pa, T = 3.592 s. The cancer cells are modeled as: (A) PANC-1which is a common cell-line of pancreatic cancer, B) MIA-PaCa-2The cancer cells and stromal cells were all modelled as incompressible elastic material where Young's modulus of fibroblasts is set to 650, 1250, and 2500 Pa [23, 48–50], for PANC-1 is set to 2,400 Pa, and for MIA-PaCa-2 is set to 500 Pa [51–53]. Among two cancer cell lines of pancreas tumors, PANC-1 and MIA-PaCa-2 which have significant differences in phenotype characteristics, we study both where PNAC-1 has been reported to be more invasive than MIA-PaCa2 [3, 4, 53]. The viscoelasticity behavior of the ECM was modeled using the viscoelastic material using

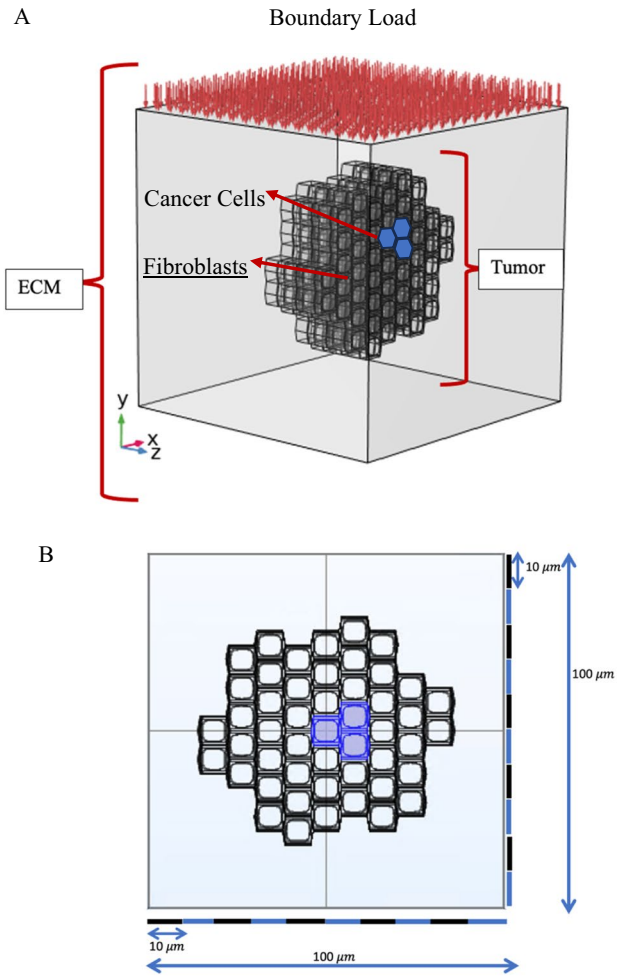

Fig. 8 In silico model of the pancreas tumor tissue containing stromal cells and three tumor cells, and ECM. The boundary load of 1,300 Pa was applied onto the system represented by the red arrows. A) A 3D model is shown, B) A 2D view is presented with details about geometry of the model

the Standard Linear Model [23, 30–32, 46, 47]. The model is represented by a purely viscous damper with viscosity η and by a purely elastic spring with modulus E in parallel, relating stress (σ) and strain (ε) [23, 30–32], shown in Eq. (1):

$$\sigma(t) = E\varepsilon(t) + \eta\frac{d\varepsilon(t)}{dt} \tag{1}$$

The relaxation time, t*, of a viscoelastic material undergone stress due to Eq. 1 is given by Eq. 2 [23, 30–32, 54–56]:

$$t^* = \frac{\eta}{E} \tag{2}$$

The stress components are then computed and applied to calculate the von Mises stress (σ_{VM}), normally referred to as the effective stress [3, 23, 42–53], which is calculated with Eq. 3:

$$\sigma_{VM} = \left\{ {}^1\!/_2 \left[(\sigma_{xx} - \sigma_{yy})^2 + (\sigma_{xx} - \sigma_{zz})^2 + (\sigma_{yy} - \sigma_{zz})^2 + 6\left(\sigma_{xy}^2 + \sigma_{xz}^2 + \sigma_{yz}^2\right) \right] \right\}^{1/2} \tag{3}$$

Von Mises stress is a measure of the effective stress, including normal stresses (x, y, and z) and the shear stresses that act on a material, which is experienced by a material.

A MATLAB code (MATLAB v. R2021b) is applied to generate the geometry of the sinusoidal surface of cells. Model geometries are exported to the finite-element method solver via COMSOL MULTIPHYSICS v. 5.6 (COMSOL AB, Stockholm, Sweden). The tumor tissue geometry (including cancer cells and stromal cells) was then enclosed by including ECM. The cancer cells were placed at the center of tumor surrounded by stromal cells (Figs. 8A and B). All cellular components and ECM are assigned with material properties and mesh specifications. A boundary load was added to the model to represent the blood pressure in capillaries as 10 mmHg (~ 1300 Pa) as seen in Fig. 8A [57]. A computational mesh was applied for the ECM and the entire tumor. The tumor contained 464,690 tetrahedral elements while ECM contained 991,925 tetrahedral elements. The computational results for the stresses are determined and examined for independence of mesh density. The models are solved using a stationary solver where simulations were performed on a Dell PRECISION, 16 processor computer, with 128 GB RAM. The postprocessed results obtained for stresses are gathered using post-processing features found in COMSOL MULTIPHYSICS v. 5.6 package. Post-processed results for stresses experienced by tumor tissue components are exported to MATLAB_R2021b for postprocessing.

Acknowledgements
We acknowledge support from University of Wisconsin-Milwaukee-Graduate School Advanced Opportunity Program (AOP), University of Wisconsin-Milwaukee (project number: 101-193590-AAI3246-4), and Office of Undergraduate Research (OUR) for proving Support for Undergraduate Research Fellows.

Author contributions
Conception and design: Mahsa Dabagh; acquisition of data: Morgan Connaughton and Mahsa Dabagh; analysis and interpretation of data: Morgan Connaughton and Mahsa Dabagh; literature search: Morgan Connaughton and Mahsa Dabagh; drafting the article: Mahsa Dabagh and Morgan Connaughton; critically revising the article: Mahsa Dabagh; reviewed submitted version of manuscript: Mahsa Dabagh; approved the final version of the manuscript on behalf of all the authors: Mahsa Dabagh; study supervision: Mahsa Dabagh; funds collection: Mahsa Dabagh.

Funding
NSF (Award Number: 2229652). University of Wisconsin-Milwaukee-Discovery and Innovation Grant (Project Number: 101-199821-4-101X433) and University of Wisconsin-Milwaukee (Project Number: 101-193590-AAI3246-4).

Availability of data and materials
The datasets used and/or analyzed during the current study available from the corresponding author on reasonable request.

Declarations

Ethical approval and consent to participate
No human studies were carried out by the authors for this article. No animal studies were carried out by the authors for this article.

Competing interests
The author Mahsa Dabagh declares that they had no financial, professional or personal conflict of interest. The author Morgan Connaughton declares that they had no financial, professional or personal competing interests.

Received: 23 December 2023 Accepted: 6 August 2024
Published online: 30 August 2024

References

1. Cancer Facts & Figures 2023. Atlanta: American Cancer Society, Inc. 2022.
2. Delle Cave D, Rizzo R, Sainz B, Gigli G, del Mercato LL, Lonardo E. The revolutionary roads to study cell-cell interactions in 3D In Vitro pancreatic cancer models. Cancers. 2021;13:930. https://doi.org/10.3390/cancers13040930.
3. Pednekar KP, Heinrich MA, van Baarlen J, Prakash J. Novel 3D tissues mimicking the fibrotic stroma in pancreatic cancer to study cellular interactions and stroma-modulating therapeutics. Cancers. 2021;13:5006. https://doi.org/10.3390/cancers13195006.
4. Gündel B, Liu X, Löhr M, Heuchel R. Pancreatic ductal adenocarcinoma: preclinical in vitro and ex vivo models. Front Cell Dev Biol. 2021;9:741162. https://doi.org/10.3389/fcell.2021.741162.
5. Manoukian P, Bijlsma MF, van Laarhoven HW. The cellular origins of cancer-associated fibroblasts and their opposing contributions to pancreatic cancer growth. Front Cell Dev Biol. 2021;9:743907. https://doi.org/10.3389/fcell.2021.743907.
6. Jiang B, Zhou L, Lu J, Wang Y, Liu C, You L, Guo J. Stroma-targeting therapy in pancreatic cancer: one coin with two sides? Front Oncol. 2020;10:576399. https://doi.org/10.3389/fonc.2020.576399.
7. Hu X, Xia F, Lee J, Li F, Lu X, Zhuo X, Nie G, Ling D. Tailor-made nanomaterials for diagnosis and therapy of pancreatic ductal adenocarcinoma. Adv Sci. 2021;8:2002545. https://doi.org/10.1002/advs.202002545.
8. Tanaka H, Kano MR. Stromal barriers to nanomedicine penetration in the pancreatic tumor microenvironment. Cancer Sci. 2018;109:2085–92. https://doi.org/10.1111/cas.13630.
9. Osuna de la Peña D, et al. Bioengineered 3D models of human pancreatic cancer recapitulate in vivo tumour biology. Nat Commun. 2021;12:5623. https://doi.org/10.1038/s41467-021-25921-9.
10. Heinrich M, et al. Translating complexity and heterogeneity of pancreatic tumor: 3D in vitro to in vivo models. Adv Drug Delivery Rev. 2021;174:265–93. https://doi.org/10.1016/j.addr.2021.04.018.
11. Su T, et al. Polymer nanoparticle-assisted chemotherapy of pancreatic cancer. Ther Adv Med Oncol. 2020;12:1–33. https://doi.org/10.1177/1758835920915978.
12. Sahai E, et al. A framework for advancing our understanding of cancer- associated fibroblasts. Nat Rev. 2020;20:174. https://doi.org/10.1038/s41568-019-0238-1.
13. Dubiella C, Pinch BJ, Koikawa K, et al. Sulfopin is a covalent inhibitor of Pin1 that blocks Myc-driven tumors in vivo. Nat Chem Biol. 2021;17:954–63. https://doi.org/10.1038/s41589-021-00786-7.
14. Kokkinos J, et al. Ex vivo culture of intact human patient derived pancreatic tumor tissue. Sci Rep. 1944;2021:11. https://doi.org/10.1038/s41598-021-81299-0.
15. Bhattacharyya S, et al. Acidic fibroblast growth factor underlies microenvironmental regulation of MYC in pancreatic cancer. J Exp Med. 2020;217:e20191805. https://doi.org/10.1084/jem.20191805.
16. Kunjachan S, et al. Author correction: selective priming of tumor blood vessels by radiation therapy enhances nanodrug delivery. Sci Rep. 2020;10:15344. https://doi.org/10.1038/s41598-020-72253-7.
17. Levayer R. Solid stress, competition for space and cancer: the opposing roles of mechanical cell competition in tumour initiation and growth. Sem Can Biol. 2020;63:69–80.
18. Bacevic K, Noble R, Soffar A, Wael Ammar O, Boszonyik B, Prieto S, Vincent C, Hochberg ME, Krasinska L, Fisher D. Spatial competition constrains resistance to targeted cancer therapy. Nat Commun. 2017;8:1995.
19. Shirinifard A, Gens JS, Zaitlen BL, Popławski NJ, Swat M, Glazier JA. 3D multi-cell simulation of tumor growth and angiogenesis. PLoS ONE. 2009;4:e7190. https://doi.org/10.1371/journal.pone.0007190.
20. Fritz M, et al. Analysis of a new multispecies tumor growth model coupling 3D phase-fields with a 1D vascular network. Nonlinear Anal Real World Appl. 2021;61:103331. https://doi.org/10.1016/j.nonrwa.2021.103331.
21. Iranmanesh F, Nazari ML. Finite element modeling of avascular tumor growth using a stress-driven model. J Biomech Eng. 2017;139:081009. https://doi.org/10.1115/1.4037038.
22. Hidrovo I, et al. Experimental method and statistical analysis to fit tumor growth model using SPECT/CT imaging: a preclinical study. Quant Imaging Med Surg. 2017;7:29. https://doi.org/10.21037/qims.2017.06.05.

23. Murphy H, Jaafari H, Dobrovolny HM. Differences in predictions of ODE models of tumor growth: a cautionary example. BMC Cancer. 2016;16:163. https://doi.org/10.1186/s12885-016-2164-x.
24. Watanabe Y, Dahlman EL, Leder KZ, Hui SK. A mathematical model of tumor growth and its response to single irradiation. Theor Biol Med Model. 2016;13:6. https://doi.org/10.1186/s12976-016-0032-7.
25. Ponce Bobadilla AV, Doursat R, Amblard F. An agent-based model of avascular tumor growth. Proc Eur Conf Artificial Life. 2015. https://doi.org/10.7551/978-0-262-33027-5-ch114.
26. Jiang Y, Pjesivac-Grbovic J, Cantrell C, Freyer J. A multiscale model for avascular tumor growth. Biophys J. 2005;89:3884. https://doi.org/10.1529/biophysj.105.060640.
27. Fritz M, Jha PK, Köppl T, Oden JT, Wohlmuth B. Analysis of a new multispecies tumor growth model coupling 3D phase-fields with a 1D vascular network. Nonlinear Anal Real World Appl. 2021. https://doi.org/10.1016/j.nonrwa.2021.103331.
28. Langer EM, Allen-Petersen BL, King SM, Kendsersky ND, Turnidge MA, Kuziel GM, Riggers R, Samatham R, Amery TS, Jacques SL, Sheppard BC, Korkola JE, Muschler JL, Thibault G, Chang YH, Gray JW, Presnell SC, Nguyen DG, Sears RC. Modeling tumor phenotypes In Vitro with three-dimensional bioprinting. Cell Rep. 2019;26:608-623.e6. https://doi.org/10.1016/j.celrep.2018.12.090.
29. Patmanidis S, Charalampidis A, Kordonis L, Mitsis G, Papavassilopoulos G. Tumor growth modeling: parameter estimation with maximum likelihood methods. Comput Methods Programs Biomed. 2018;160:1–10. https://doi.org/10.1016/j.cmpb.2018.03.014.
30. Medha B, Chandana D, Sowmya V, Godfrey W, Kaushal G, Dhar J. Tumor Growth Modeling and Estimation of Changes with Respect to Cytotoxic Drugs. TENCON-IEEE Region 10 Conference (TENCON), 2019; 1053–1058. https://doi.org/10.1109/TENCON.2019.8929486.
31. Metzcar J, Wang Y, Heiland R, Macklin P. A review of cell-based computational modeling in cancer biology. American society of clinical oncology. JCO Clin Cancer Inform. 2019;3:1–13. https://doi.org/10.1200/CCI.18.00069.
32. Jafari Nivlouei S, Soltani M, Carvalho J, Travasso R, Salimpour MR, Shirani E. Multiscale modeling of tumor growth and angiogenesis: evaluation of tumor-targeted therapy. PLoS Comput Biol. 2021;17:e1009081. https://doi.org/10.1371/journal.pcbi.100908.
33. Taufalele P, Wang W, Simmons A, Southard-Smith A, Chen B, Greenlee J, King M, Lau K, Hassane D, Bordeleau F, Reinhart-King CA. Matrix stiffness enhances cancer-macrophage interactions and M2-like macrophage accumulation in the breast tumor microenvironment. Acta Biomater. 2022. https://doi.org/10.1016/j.actbio.2022.04.031.
34. Hope JM, Dombroski JA, Pereles RS, Reinhart-King CA, King M. Fluid shear stress enhances T cell activation through Piezo1. BMC Biol. 2022;20:61. https://doi.org/10.1186/s12915-022-01266-7.
35. Greenlee JD, Liu K, Lopez-Cavestany M, King MR. Piezo1 Mechano-activation is augmented by resveratrol and differs between colorectal cancer cells of primary and metastatic origin. Molecules. 2022;27:5430. https://doi.org/10.3390/molecules27175430.
36. Connaughton M, Dabagh M. Modeling physical forces experienced by cancer and stromal cells within different organ-specific tumor tissue. IEEE J Trans Eng Health Med. 2024;12:413–34. https://doi.org/10.1109/JTEHM.2024.3388561.
37. Liu T, Han C, Wang S, Fang P, Ma Z, Xu L, et al. Cancer-associated fibroblasts: an emerging target of anti-cancer immunotherapy. J Hematol Oncol. 2019;12(1):86. https://doi.org/10.1186/s13045-019-0770-1.
38. Ernsting MJ, Hoang B, Lohse I, Undzys E, Cao P, Do T, et al. Targeting of metastasis-promoting tumor-associated fibroblasts and modulation of pancreatic tumor-associated stroma with a carboxymethylcellulose-docetaxel nanoparticle. J Control Release. 2015;206:122–30. https://doi.org/10.1016/j.jconrel.2015.03.023.
39. Jiang B, Zhou L, Lu J, Wang Y, Liu C, You L, et al. Stroma-targeting therapy in pancreatic cancer: one coin with two sides? Front Oncol. 2020;10:576399. https://doi.org/10.3389/fonc.2020.576399.
40. Gao S, Yang D, Fang Y, Lin X, Jin X, Wang Q, et al. Engineering nanoparticles for targeted remodeling of the tumor microenvironment to improve cancer immunotherapy. Theranostics. 2019;9(1):126–51. https://doi.org/10.7150/thno.29431.
41. Tang L, Mei Y, Shen Y, He S, Xiao Q, Yin Y, et al. Nanoparticle-mediated targeted drug delivery to remodel tumor microenvironment for cancer therapy. Int J Nanomed. 2021;16:5811–29. https://doi.org/10.2147/IJN.S321416.
42. Ebben A, Dabagh M. Mechanotransduction in endothelial cells in vicinity of cancer cells. Cell Mol Bioeng. 2022. https://doi.org/10.1007/s12195-022-00728-w.
43. Dabagh M, Jalali P, Butler PJ, Randles A, Tarbell JM. Mechanotransmission in endothelial cells subjected to oscillatory and multidirectional shear flow. J R Soc Interface. 2017;14:20170185.
44. Dabagh M, Jalali P, Butler PJ, Tarbell JM. Shear-Induced force transmission in a multicomponent, multicell model of endothelium. J Royal Soc Interface. 2014;11:20140431.
45. Alonso A, Ebben A, Dabagh M. Impact of disturbed flow and arterial stiffening on mechanotransduction in endothelial cells. Biomech Model Mechanobiol. 2023. https://doi.org/10.1007/s10237-023-01743-0.
46. Rice A, Cortes E, Lachowski D, et al. Matrix stiffness induces epithelial–mesenchymal transition and promotes chemoresistance in pancreatic cancer cells. Oncogenesis. 2017;6:e352. https://doi.org/10.1038/oncsis.2017.54.
47. Kpeglo D, Hughes MD, Dougan L, Haddrick M, Knowles MA, Evans SD, Peyman SA. Modeling the mechanical stiffness of pancreatic ductal adenocarcinoma. Matrix Biol Plus. 2022;14:100109. https://doi.org/10.1016/j.mbplus.2022.100109.
48. Efremov YuM, Lomakina ME, Bagrov DV, Makhnovskiy PI, Alexandrova AY, Kirpichnikov MP, Shaitan KV. Mechanical properties of fibroblasts depend on level of cancer transformation. Biochimica et Biophys Acta (BBA) Mol Cell Res. 2024;1842:1013–9. https://doi.org/10.1016/j.bbamcr.2014.01.032.
49. Jafari Nivlouei S, Soltani M, Carvalho J, Travasso R, Salimpour MR, Shirani E. Multiscale modeling of tumor growth and angiogenesis: evaluation of tumor-targeted therapy. PLoS Comput Biol. 2021;17:e1009081.
50. Thomas G, Burnham NA, Camesano TA, Wen Q. Measuring the mechanical properties of living cells using atomic force microscopy. J Vis Exp. 2013;2023(76):e50497. https://doi.org/10.3791/50497.
51. Quan FS, Kim KS. Medical applications of the intrinsic mechanical properties of single cells. Acta Biochim Biophys Sin. 2016;48(10):865–71. https://doi.org/10.1093/abbs/gmw081.

52. Gradiz R, Silva HC, Carvalho L, Botelho MF, Mota-Pinto A. MIA PaCa-2 and PANC-1—pancreas ductal adenocarcinoma cell lines with neuroendocrine differentiation and somatostatin receptors. Sci Rep. 2016. https://doi.org/10.1038/srep21648.
53. Nguyen AV, Nyberg KD, Scott MB, Welsh AM, Nguyen AH, Wu N, Hohlbauch SV, Geisse NA, Gibb EA, Robertson AG, Donahue TR, Rowat AC. Stiffness of pancreatic cancer cells is associated with increased invasive potential. Integr Biol (Camb). 2016;8(12):1232–45. https://doi.org/10.1039/c6ib00135a.
54. Ghigo AR, Wang XF, Armentano R, Lagree PY, Fullana JM. Linear and nonlinear viscoelastic arterial wall models: application on animals. J Biomech Eng. 2017. https://doi.org/10.1115/1.4034832.
55. Valdez-Jasso D, Bia D, Zócalo Y, Armentano R, Haider M, Olufsen M. Linear and nonlinear viscoelastic modeling of aorta and carotid pressure-area dynamics under in vivo and ex vivo conditions. Ann Biomed Eng. 2011;39:1438–56. https://doi.org/10.1007/s10439-010-0236-7.
56. Chaudhuri O, Cooper-White J, Janmey PA, Mooney DJ, Shenoy VB. Effects of extracellular matrix viscoelasticity on cellular behaviour. Nature. 2020;584(7822):535–46. https://doi.org/10.1038/s41586-020-2612-2.
57. Shore AC. Capillaroscopy and the measurement of capillary pressure. Br J Clin Pharmacol. 2000;50:501–13. https://doi.org/10.1046/j.1365-2125.2000.00278.x.
58. Provenzano PP, Cuevas C, Chang AE, Goel VK, Von Hoff DD, Hingorani SR. Enzymatic targeting of the stroma ablates physical barriers to treatment of pancreatic ductal adenocarcinoma. Cancer Cell. 2012;20(21):418–29. https://doi.org/10.1016/j.ccr.2012.01.007.
59. Ligorio M, Sil S, Malagon-Lopez J, Nieman LT, Misale S, Di Pilato M, Ebright RY, Karabacak MN, Kulkarni AS, Liu A, Jordan NV, Franses JW, Philipp J, Kreuzer J, Desai N, Arora KS, Rajurkar M, Horwitz E, Neyaz A, Tai E, Magnus NKC, Vo KD, Yashaswini CN, Marangoni F, Boukhali M, Fatherree JP, Damon LJ, Xega K, Desai R, Choz M, Bersani F, Langenbucher A, Thapar V, Morris R, Wellner UF, Schilling O, Lawrence MS, Liss AS, Rivera MN, Deshpande V, Benes CH, Maheswaran S, Haber DA, Fernandez-Del-Castillo C, Ferrone CR, Haas W, Aryee MJ, Ting DT. Stromal microenvironment shapes the intratumoral architecture of pancreatic cancer. Cell. 2019;178:160–17527. https://doi.org/10.1016/j.cell.2019.05.012.
60. Elahi-Gedwillo KY, Carlson M, Zettervall J, Provenzano PP. Antifibrotic therapy disrupts stromal barriers and modulates the immune landscape in pancreatic ductal adenocarcinoma. Cancer Res. 2019;79:372–86. https://doi.org/10.1158/0008-5472.CAN-18-1334.
61. Subrahmanyam N, Ghandehari H. Harnessing extracellular matrix biology for tumor drug delivery. J Pers Med. 2021;11(2):88. https://doi.org/10.3390/jpm11020088.
62. McGuigan A, Kelly P, Turkington RC, Jones C, Coleman HG, McCain RS. Pancreatic cancer: a review of clinical diagnosis, epidemiology, treatment and outcomes. World J Gastroenterol. 2018;24(43):4846–61. https://doi.org/10.3748/wjg.v24.i43.4846.
63. Wang S, Zheng Y, Yang F, Zhu L, Zhu XQ, Wang ZF, Wu XL, Zhou CH, Yan JY, Hu BY, Kong B, Fu DL, Bruns C, Zhao Y, Qin LX, Dong QZ. The molecular biology of pancreatic adenocarcinoma: translational challenges and clinical perspectives. Signal Trans Target Ther. 2021. https://doi.org/10.1038/s41392-021-00659-4.
64. Lyu Y, Xiao Q, Li Y, Wu Y, He W, Yin L. "Locked" cancer cells are more sensitive to chemotherapy. Bioeng Transl Med. 2019;4:e10130. https://doi.org/10.1002/btm2.10130.
65. Kumar S, Weaver VM. Mechanics. malignancy, and metastasis: the force journey of a tumor cell. Cancer Metastasis Rev. 2009;28(1–2):113–27. https://doi.org/10.1007/s10555-008-9173-4.
66. Lange JR, Fabry B. Cell and tissue mechanics in cell migration. Exp Cell Res. 2013;319:2418–23. https://doi.org/10.1016/j.yexcr.2013.04.023.
67. Stine P, Else H, Ivana N. Cell volume regulation in epithelial physiology and cancer. Front Physiol. 2013. https://doi.org/10.3389/fphys.2013.00233.
68. Makki J. Diversity of Breast carcinoma: histological subtypes and clinical relevance. Clin Med Insight Pathol. 2015;8:CPath.S31563. https://doi.org/10.4137/cpath.s31563.
69. Adjo Aka J, Lin SX. Comparison of functional proteomic analyses of human breast cancer cell lines T47D and MCF7. PLoS ONE. 2012;7(2):e31532. https://doi.org/10.1371/journal.pone.0031532.
70. Nallanthighal S, Heiserman JP, Cheon DJ. The role of the extracellular matrix in cancer stemness. Front Cell Dev Biol. 2019. https://doi.org/10.3389/fcell.2019.00086.
71. Morishita K, Watanabe K, Ichijo H. Cell volume regulation in cancer cell migration driven by osmotic water flow. Cancer Sci. 2019;110(8):2337–47. https://doi.org/10.1111/cas.14079.

Publisher's Note